Application of Fragment Molecular Orbital Method to investigate dopamine receptors

Jokūbas Preikša, Paweł Śliwa*

Faculty of Chemical Engineering and Technology, Cracow University of Technology, Warszawska 24 St, 31–155 Cracow, Poland

Article history:
Received 12 September 2019
Received in revised form
27 October 2019
Accepted 29 October 2019
Available online 31 October 2019

Abstract
GPCRs are a vast family of seven-domain transmembrane proteins. This family includes dopamine receptors (D_1, D_2, D_3, D_4, and D_5), which mediate the variety of dopamine-controlled physiological functions in the brain and periphery. Ligands of dopamine receptors are used for managing several neuropsychiatric disorders, including bipolar disorder, schizophrenia, anxiety, and Parkinson's disease. Recent studies have revealed that dopamine receptors could be part of multiple signaling cascades, rather than of a single signaling pathway. For these targets, a variety of experimental and computational drug design techniques are utilized. In this work, dopamine receptors D_2, D_3, and D_4 were investigated using molecular dynamic method as well as computational *ab initio* Fragment Molecular Orbital method (FMO), which can reveal atomistic details about ligand binding. The results provided useful insights into the significances of amino acid residues in ligand binding sites. Moreover, similarities and differences between active-sites of three studied types of receptors were examined.

Keywords: Fragment Molecular Orbital, Molecular Dynamic, Dopamine receptors

Introduction

Dopamine is a neurotransmitter and produces a particular effect when binding to specific receptors located in a cell membrane. These receptors belong to an evolutionary related G-protein coupled receptor (GPCR) group. Dopamine receptors are structurally built from seven-pass-transmembrane domains, and are subdivided into two sub-groups (D_1-like, and D_2-like) [1, 2]. Therefore, the D_1-like sub-group consists of D_1 and D_5 receptors, whereas D_2-like receptors are D_2, D_3, and D_4 [3]. Apart from having different functionalities as sub-groups, and as a specific type of dopamine receptor, these GPCRs are known to signal in different pathways [4]. For example, D_2 receptor can signal not only through cAMP pathway, but also through calcium ion cascade, β-arrestin, and transactivation of other receptors, such as receptor tyrosine kinase. This leads to biased signaling which is an attractive field of research in modern biochemistry [3,5–12].

Dopamine receptor ligands are compounds that bind to dopamine receptors as either agonists or antagonists. However, the expanding realization of biased dopamine receptors' signaling mechanisms provides a theoretical framework for the investigation of specific ligands that support partial activation or inhibition of the receptor [13]. Owing to the specific interactions biased ligands support a certain conformation, and are capable of fully signaling one dopamine receptor pathway while displaying little to no activity on the other [14]. The search for such compounds is a complicated task, so numerous computational techniques are being exploited to aid scientific research [15, 16].

Fragment molecular orbital (FMO) is a computational ab initio method, which uses quantum mechanical calculations to investigate chemical systems. Ab initio computations are recognized as very accurate, however also as very demanding techniques. To counter the latter problem, fragmentation techniques were introduced [17], so that the advantages of parallel processing could be utilized [18–22]. Using FMO it is possible to execute calculations for energy, energy gradient, dipole moment, etc. [23]. The calculation of FMO consists of the following steps: a) fragmentation (assignment of atoms to the specific fragments), b) fragmentation of the self-consistent field calculations in the embedding polarizable potential, so that fragments polarize each other in self-consistent manner, accounting for inter-fragment load transfer and other quantum effects, c) fragment pair, triple and quadruple self-consistent field calculations, transferring inter-fragmental charge, and d) assessment of total property (energy, gradient, etc.) [24]. As a result of FMO calculations, one obtains pair interaction energy decomposition analysis (PIEDA). PIEDA enables a very thorough analysis of the interaction energy contributions and their couplings (e.g., polarization coupling and dispersion). Pair interaction energies (PIE) are decomposed as:

$$\Delta E_{IJ} = \Delta E_{IJ}^{ES} + \Delta E_{IJ}^{EX} + \Delta E_{IJ}^{CT+mix} + \Delta E_{IJ}^{DI} + G_{IJ}^{SOLV} \quad (1)$$

where the terms of the equation are electrostatic (ES), exchange-repulsion (EX), charge transfer and higher order

*Corresponding author: psliwa@chemia.pk.edu.pl

terms (CT+mix), dispersion (DI), and solvation (SOLV) terms. The electrostatic and charge transfer contributions predominate in salt-bridge, hydrogen bond, and polar interactions, whereas dispersion term usually refers to hydrophobic interactions. The identification of hydrophobic interactions for biomolecular systems is essential. The exchange-repulsion term is the quantum mechanical term that quantifies the repulsion between electrons. In the case of the ligand-protein complex, the PIE equation gives "strength" of the ligand-protein residue interaction [25]. This leads to major applicability of this method in big biological systems and gaining insight into more specific protein-ligand interactions [19, 21, 33–41, 25–32].

Materials and Methods

Structure preparation and MD simulation

For the FMO analysis D_2, D_3, and D_4 receptors were selected, for which X-ray crystal structures are deposited in Protein Data Bank (PDB ID: 6CM4, 3PBL, 5WIV respectively). The ligands used in the calculations were the ligands co-crystalized with proteins (Figure 1). Risperidone is an antagonist of the D_1-like (D_1, and D_5) as well as the D_2 family (D_2, D_3 and D_4) receptors, with 70-fold selectivity for the D_2 family. Eticlopride is a selective dopamine antagonist that acts mainly on D_2-like receptors. Nemonapride is an atypical antipsychotic and acts as a D_2, D_3 and D_4 receptors antagonist, and is also a potent 5-HT_{1A} receptor agonist [42].

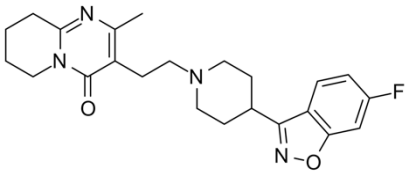

D_2: Risperidone
K_i [D_1] = 244 nM
K_i [D_2] = 3.57 nM
K_i [D_3] = 3.6 nM
K_i [D_4] = 4.66 nM

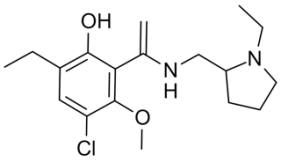

D_3: Eticlopride
K_i [D_2] = 0.26 nM
K_i [D_3] = 0.11 nM
K_i [D_4] = 70.4 nM

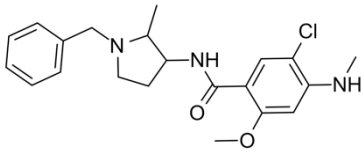

D_4: Nemonapride
K_i [D_4] = 0.21 nM

Figure 1. Structures of ligands co-crystalized with dopamine receptors [42]. Affinity values for receptors with which they form complexes in crystals are bold

The molecular dynamic simulations (100 ns) were performed using NAMD [43]. The ligands were parameterized using automatic CHARMM General Force Field (CgenFF) generator [44]. For the preparation of the protein-ligand complexes, VMD extension tool QwikMD was used [44]. Using this program phosphatidylcholine (POPC) membrane was created based on the positioning estimated from the PPM web server (http://opm.phar.umich.edu/server.php, accessed 30-06-2019) [45]. Before running the simulation, the explicit solvent was added with a NaCl concentration of 0.15 mol/L. The molecular dynamic simulation was performed in four steps: Minimization (2000 steps of 2 fs), Annealing (600 steps of 2 fs), Equilibration (500000 steps of 2 fs, T=300 K), and MD (50000000 steps of 2 fs, T=300 K, p=1 atm).

The MD trajectories analysis and structure clustering were performed using MD Movie Tool from UCSF Chimera v.1.13.1 [46]. From the most populated clusters, their centroids were selected for further calculations, whereas for D_2 was two, for D_3 three, while for D_4 four representative structures.

FMO calculations

FMO input files were prepared using Facio software v. 22.1.1 [37, 47]. The fragmentation of complexes under study was generated mostly automatically, however, to obtain all the amino acid residues as a single fragment, some bond detachments had to be done manually. Then, using the FMO methodology, the PIE between ligand and binding site amino acids (less than 4.5 Angstrom from the ligand) was calculated.

In this work, computations were performed on the second-order Möller-Plesser perturbation (MP2) level of theory with the 6-31G* basis set (FMO-MP2/6-31G*) [18–22] and polarizable continuum model (PCM) [48]. Calculations were performed using GAMESS [18] on the super-computer Prometheus employing 24 CPUs.

In order to evaluate nature of interactions, based on PIEDA results, the percentage of the sum of absolute values of charge transfer and electrostatic contributions in the total attraction energy was calculated as follows [36]:

$$\%E^{ES+CT} = \frac{|E^{ES}|+|E^{CT+mix}|}{|E^{ES}|+|E^{CT+mix}|+|E^{DI}|} \times 100\% \qquad (2)$$

In this way, the value of 100% means purely polar interaction, and 0% can be interpreted as fully hydrophobic interaction.

In this work, the PDB notation of amino acid residues is used. In the case of comparison between different receptors, dual names were used: the PDB numbering and the scheme proposed by Ballesteros–Weinstein [49], where a one-letter amino acid

symbol and the sequence-based generic GPCR residue number are used, e.g. D3.32 mean aspartic acid located at position 32 in the third helix.

Results and Discussion

Clustering results of the molecular dynamics trajectories

Choosing the appropriate molecular structure is probably the most important and the most difficult step of FMO calculations. There is no clear answer which preparation approach or optimization method is the best. Until now, we have used docking and QMMM optimization [35, 36, 50]. This approach was relatively time-consuming, which is why we have attempted to use the molecular dynamics method, which with the current capabilities of GPUs is definitely a faster approach. In turn, the disadvantage of this method may be that the result of the MD calculations is a trajectory i.e. a huge set of structures, often energetically similar. The generation of smaller subsets, as a result of clustering according to a selected rule (RMSD of protein, RMSD of ligand, energy, etc.) allows for a significant reduction of this number. Usually, the most populated cluster (set of structures) is considered the most probable. However, if we obtain several clusters of similar numbers, we must take them all into account. In the current study, using the approach described above, we have obtained two, three and four representative structures of ligand-receptor complexes for D_2, D_3 and D_4 receptors respectively.

In the case of D_2 receptor the calculated absolute values of total interaction energy (the sum of pair interaction energies between ligand and residues of bonding pocket) were only slightly bigger for the first complex (D_{2I}), however, for D_{2II} one additional attractive interaction with VAL-11 was observed (Figure 2). The FMO results indicated that interactions with all thirteen residues of binding site stabilized the complex. Interestingly, calculations revealed presence of up to seven molecules of water, which were employed to the ligand binding.

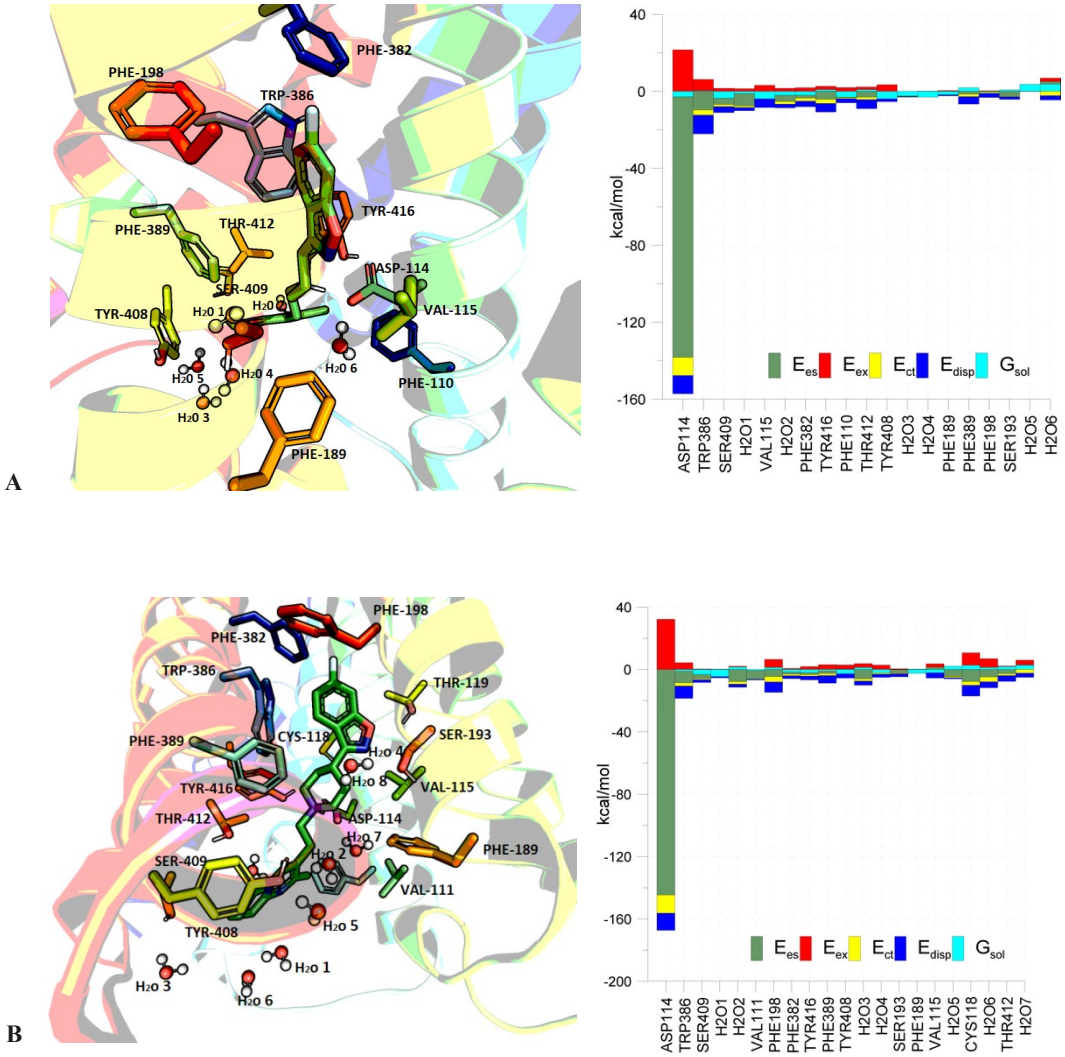

Figure 2. Representation of D2 receptor active sites. Centroids of the first (A) and second (B) clusters obtained on the basis of the MD trajectory clustering. The FMO-PIEDA energy analysis of those complexes

In the case of D_3 receptor (see Supplementary information: Figure S1), based on FMO calculations, 23 amino acid residues that can interact with the ligand were identified. However, only ten of them were permanently involved in the ligand binding, which seven of them interacted attractively (ASP-110, VAL-107, TYR-365, PHE-345, VAL189, PHE-188 and PHE-346), two repulsively (TYR-373 and THR-115) and one could both (SER-192). In addition, there may be up to 5 water molecules at the D_3 receptor binding site that also interacts with the ligand. Looking for differences between selected structures, we noted that, in the representative structure of the second cluster (D_{3II}) there were additional interactions between the ligand and VAL-86, PHE-197, HIS-349, VAL-350, compared to the D_{3I} complex. While the D_{3III} complex, in the binding site, additionally contained residues such as ILE-183, HIS-349 and VAL-350, but TRP-342 was missing. Finally, FMO calculations indicated that the ligand was most strongly bound in the D_{3II} complex, although the ligand binding energy in D_{2I} is only 6% lower.

Four representative structures of ligand-receptor complexes have been selected for the D_4 receptor (Supplementary information: Figure S2). As before, FMO calculations indicated that the receptor binding pocket could be formed by 21 amino acid residues, however, only with ten of them the ligand interacted throughout the MD simulation. The complex, in this case "inactive", was stabilized by contacts with ASP-115, MET-112, VAL-116, PHE-91, PHE-410, TRP-407, VAL-87, SER-196, TYR-192 and LEU-111, while it was destabilized mainly by interaction with ARG-186. The most stable structure was D_{4III}, while the least was D_{4I}. The lowest energy of the latter was due to formation of strong repulsive interactions between ligand and threonines numbers 120 and 434, but also might be the result of an energetically weaker salt bridge.

As one can see, the task was quite difficult to solve, so the logical choice should be to choose the structure most represented. For those, based on FMO results, the binding pockets of three dopamine receptors were compared in the next paragraph.

The characterization of binding pockets of dopamine receptors using the FMO calculation

The list of amino acid residues, crystalline water molecules employed to ligand binding by dopamine receptors, and the pair interaction energies from FMO calculations are presented in Table 1. It is known that the molecules tested are very active dopamine D_2-type receptor antagonists, i.e. three complexes discussed above are inactive protein conformations. All of the structures are characterized by strong electrostatic interaction between aspartate ion (ASP 3.32) and quaternary ammonium cation of the ligand. Pair interaction energies with D_2, D_3, and D_4 are -138.4, -125.15 and -117.6 kJ/mol, respectively. Because the salt bridge strength is geometrically dependent, as was previously proved by Kurczab et al [51], these differences could be associated with that effect. Secondly, the water molecules near aspartate were observed, which could affect the electron density of interacting parts (see Figure 2A, and Supplementary information).

Generally, according to PIEDA calculations, besides D_2, dopamine receptors interact with their ligands in both hydrophobic and hydrophilic manner. Although the complexes under study contain different ligands, there was a great similarity of binding pockets in this series of dopamine receptors. That is, the antagonistic effect of ligands on various D_2-like receptors could be associated with a similar mechanism. All ligands interacted with characteristic residues, also for other aminergic receptors, from helix 3, 5 and 6. The results of FMO/PIEDA also indicated subtle differences, especially for the D_4 receptor, where the ligand interacted with residues from TMH2 instead of TMH7, as it was for D_2 and D_3.

Conclusions

The dopamine receptor-ligand complexes, namely D_2–Risperidone, D_3–Eticlopride, and D_4–Nemonapride, were investigated using molecular dynamics and fragment molecular orbital computational methods. Firstly, MD simulations were used to obtain appropriate molecular structures. Then, ligand binding sites were extracted from each cluster and subjected to interaction energy calculations with ab initio method using FMO approach. As a result, the obtained pair interaction energy decomposition analysis provided valuable insights for binding sites of different dopamine receptors.

By analysing total pair interaction energies, and comparing different clusters of the same receptor, constant amino acid residues were selected as the most important ones for the stability of the protein-ligand complex.

Moreover, by investigating the binding sites of the first clusters of each dopamine receptor type, some similarities and differences were elucidated. FMO revealed that all of the structures were stabilized by two types of interactions hydrophobic, and hydrophilic. All dopamine receptor-ligand complexes are characterized by strong electrostatic interaction between negatively charged aspartic acid residue and quaternary ammonium cation. Other residues such as tyrosine, serine increased hydrophilic stabilization.

These results are promising in further investigation of dopamine receptors either by acquiring other crystallographic structures and gaining even more accurate insight into an active centres, creating FMO based pharmacophores, carrying out virtual screenings or by performing docking techniques, and leading the innovation of novel compounds that selectively bind to the receptors, and possibly have desired biased signaling properties.

Acknowledgments

This study was supported in part by PL-Grid Infrastructure.

Table 1. Pair interaction energies between ligand and binding site residues of dopamine receptors. Attractive and repulsive interactions are highlighted in green or red, respectively. The nature of interactions by mean of the %EES+CT calculated on the basis of Eq. 2. Cells with values above 60% are blue and those below 40% purple.

Protein substructure	Res. No.	D_2			D_3			D_4		
			PIE	$\%E^{ES+CT}$		PIE	$\%E^{ES+CT}$		PIE	$\%E^{ES+CT}$
TMH2	2.57							VAL87	-5	40
	2.60							LEU90	-3	31
	2.61							PHE91	-7	45
	2.64							SER94	-3	59
TMH3	3.28	PHE110	-7	65	PHE106	-6	33	LEU111	-4	26
	3.29				VAL107	-15	94	MET112	-10	73
	3.32	ASP114	-138	94	ASP110	-125	94	ASP115	-118	93
	3.33	VAL115	-9	35				VAL116	-9	44
	3.37				THR115	6	82	THR120	10	91
ECL2								ARG 186	4	
								LEU 187	3	
TMH5	5.38	PHE189	-4	33	PHE188	-4	23	TYR192	-3	55
	5.39				VAL189	-6	53			
	5.42	SER193	-3	71	SER192	-7	70	SER196	-3	62
	5.43				SER193	4	80			
	5.46				SER196	4	64			
	5.47	PHE198	-3	31						
TMH6	6.44	PHE382	-8	64						
	6.48	TRP386	-15	56	TRP342	-8	58	TRP407	-6	52
	6.51	PHE389	-3	41	PHE345	-10	39	PHE410	-6	33
	6.52				PHE346	-3	31			
	6.55				HIS349	-3	51	HIS414	-8	76
TMH7	7.35	TYR408	-6	23	TYR365	-11	66			
	7.36	SER409	-13	72						
	7.39	THR412	-6	48						
	7.43	TYR416	-7	58	TYR373	4	34			
	H_2O^1		-10	84		-5	55		-11	84
	H_2O^2		-9	77		-4	66		-6	85
	H_2O^3		-5	91		-3	91		-5	84
	H_2O^4		-4	58		3	83		8	84
	H_2O^5		5	95		9	98			
	H_2O^6		6	77						

* TMH – transmembrane helix, ECL – extracellular loop

References

1. Beaulieu JM, Gainetdinov RR. The Physiology, Signaling, and Pharmacology of Dopamine Receptors. Pharmacol Rev. 2011;63:182–217.
2. Vallone D, Picetti R, Borrelli E. Structure and function of dopamine receptors. Neurosci Biobehav Rev. 2000;24(1):125–32.
3. Beaulieu JM, Gainetdinov RR, Caron MG. The Akt-GSK-3 signaling cascade in the actions of dopamine. Trends Pharmacol Sci. 2007;28(4):166–72.
4. Wang M, Wong AH, Liu F. Interactions between NMDA and dopamine receptors: A potential therapeutic target. Brain Res. 2012;1476:154–63.
5. Damian M, Pons V, Renault P, M'Kadmi C, Delort B, Hartmann L, et al. GHSR-D2R heteromerization modulates dopamine signaling through an effect on G protein conformation. Proc Natl Acad Sci. 2018;115(17):4501–6.
6. Dong N, Lee DWK, Sun HS, Feng ZP. Dopamine-mediated calcium channel regulation in synaptic suppression in l. Stagnalis interneurons. Channels. 2018;12(1):153–73.
7. Hasbi A, Fan T, Alijaniaram M, Nguyen T, Perreault M, O'Dowd BF, et al. Calcium signaling cascade links dopamine D1–D2 receptor heteromer to striatal BDNF production and neuronal growth. Proc Natl Acad Sci. 2009;106(50):21477–21382.
8. Hasbi A, O'Dowd BF, George SR. Heteromerization of dopamine D2 receptors with dopamine D1 or D5 receptors generates intracellular calcium signaling by different mechanisms. Curr Opin Pharmacol. 2010;10(1):93–9.
9. Iwakura Y, Nawa H, Sora I, Chao M V. Dopamine D1 receptor-induced signaling through TrkB receptors in striatal neurons. J Biol Chem. 2008;283(23):15799–806.
10. Kotecha SA, Oak JN, Jackson MF, Perez Y, Orser BA, Van Tol HHM, et al. A D2 class dopamine receptor transactivates a receptor tyrosine kinase to inhibit NMDA receptor transmission. Neuron. 2002;35(6):1111–22.
11. Marion S, Urs NM, Peterson SM, Sotnikova TD, Beaulieu J-M, Gainetdinov RR, et al. Dopamine D2 Receptor Relies upon PPM/PP2C Protein Phosphatases to Dephosphorylate Huntingtin Protein. J Biol Chem. 2014;289(17):11715–24.
12. Medvedev IO, Ramsey AJ, Masoud ST, Bermejo MK, Urs N, Sotnikova TD, et al. D 1 dopamine receptor coupling to PLCβ regulates forward locomotion in mice. J Neurosci. 2013;33(46):18125–33.
13. Luderman KD, Conroy JL, Free RB, Southall N, Ferrer M, Sanchez-Soto M, et al. Identification of positive allosteric modulators of the D 1 dopamine receptor that act at diverse binding sites S. Mol Pharmacol. 2018;94(4):1197–209.
14. Shen Y, McCorvy JD, Martini ML, Rodriguiz RM, Pogorelov VM, Ward KM, et al. D2 Dopamine Receptor G Protein-Biased Partial Agonists Based on Cariprazine. J Med Chem. 2019;62(9):4755–71.
15. Bonifazi A, Yano H, Guerrero AM, Kumar V, Hoffman AF, Lupica CR, et al. Novel and Potent Dopamine D 2 Receptor Go-Protein Biased Agonists . ACS Pharmacol Transl Sci. 2019;2(1):52–65.
16. Chun LS, Vekariya RH, Free RB, Li Y, Lin DT, Su P, et al. Structure-activity investigation of a G protein-biased agonist reveals molecular determinants for biased signaling of the D 2 dopamine receptor. Front Synaptic Neurosci. 2018;10:1–18.
17. Gordon MS, Fedorov DG, Pruitt SR, Slipchenko L V. Fragmentation methods: A route to accurate calculations on large systems. Chem Rev. 2012;112(1):632–72.
18. Fedorov DG. The fragment molecular orbital method: theoretical development, implementation in GAMESS, and applications. Wiley Interdiscip Rev Comput Mol Sci. 2017;7(6):1–17.
19. Fedorov DG, Avramov P V., Jensen JH, Kitaura K. Analytic gradient for the adaptive frozen orbital bond detachment in the fragment molecular orbital method. Chem Phys Lett. 2009;477(1–3):169–75.
20. Fedorov DG, Jensen JH, Deka RC, Kitaura K. Covalent bond fragmentation suitable to describe solids in the fragment molecular orbital method. J Phys Chem A. 2008;112(46):11808–16.
21. Fedorov DG, Kitaura K. The importance of three-body terms in the fragment molecular orbital method. J Chem Phys. 2004;120:6832–40.
22. Fedorov DG, Kitaura K. Second order Møller-Plesset perturbation theory based upon the fragment molecular orbital method. J Chem Phys. 2004;121(6):2483–90.
23. Shimamura K, Ishimura H, Kobayashi I, Kadoya R, Kurita N, Kawai K, et al. Molecular dynamics and ab initio FMO calculations on the effect of water molecules on the interactions between androgen receptor and its ligand and cofactor. 4th IGNITE Conf 2016 Int Conf Adv Informatics Concepts, Theory Appl ICAICTA 2016. 2016;1–6.
24. Fedorov DG, Kitaura K. Pair interaction energy decomposition analysis. J Comput Chem. 2007;28(1):222–37.
25. Chudyk EI, Sarrat L, Aldeghi M, Fedorov DG, Bodkin MJ, James T, et al. Exploring GPCR-ligand interactions with the fragment molecular orbital (FMO) method. Methods Mol Biol. 2018;1705:179–95.
26. Akimov A V. Nonadiabatic Molecular Dynamics with Tight-Binding Fragment Molecular Orbitals. J Chem Theory Comput. 2016;12(12):5719–36.
27. Doi H, Okuwaki K, Mochizuki Y, Mochizuki Y, Ozawa T, Yasuoka K. Dissipative particle dynamics (DPD) simulations with fragment molecular orbital (FMO) based effective parameters for 1-Palmitoyl-2-oleoyl phosphatidyl choline (POPC) membrane. Chem Phys Lett. 2017;684:427–32.

28. Gaus M, Cui Q, Elstner M. Density functional tight binding: Application to organic and biological molecules. Wiley Interdiscip Rev Comput Mol Sci. 2014;4(1):49–61.
29. Ishimura H, Tomioka S, Kadoya R, Shimamura K, Okamoto A, Shulga S, et al. Specific interactions between amyloid-B peptides in an amyloid-B hexamer with three-fold symmetry: Ab initio fragment molecular orbital calculations in water. Chem Phys Lett. 2017;672:13–20.
30. Kobayashi I, Takeda R, Suzuki R, Shimamura K, Ishimura H, Kadoya R, et al. Specific interactions between androgen receptor and its ligand: ab initio molecular orbital calculations in water. J Mol Graph Model. 2017;75:383–9.
31. Komeiji Y, Okiyama Y, Mochizuki Y, Fukuzawa K. Interaction between a Single-Stranded DNA and a Binding Protein Viewed by the Fragment Molecular Orbital Method. Bull Chem Soc Jpn. 2018;91(11):1596–605.
32. Ozawa M, Ozawa T, Ueda K. Application of the fragment molecular orbital method analysis to fragment-based drug discovery of BET (bromodomain and extra-terminal proteins) inhibitors. J Mol Graph Model. 2017;74:73–82.
33. Sawada T, Hashimoto T, Nakano H, Suzuki T, Ishida H, Kiso M. Why does avian influenza A virus hemagglutinin bind to avian receptor stronger than to human receptor? Ab initio fragment molecular orbital studies. Biochem Biophys Res Commun. 2006;351(1):40–3.
34. Simoncini D, Nakata H, Ogata K, Nakamura S, Zhang KYJ. Quality Assessment of Predicted Protein Models Using Energies Calculated by the Fragment Molecular Orbital Method. Mol Inform. 2015;34(2–3):97–104.
35. Śliwa P, Kurczab R, Bojarski AJ. ONIOM and FMO-EDA study of metabotropic glutamate receptor 1: Quantum insights into the allosteric binding site. Int J Quantum Chem. 2018;118(15):e25617.
36. Śliwa P, Kurczab R, Kafel R, Drabczyk A, Jaśkowska J. Recognition of repulsive and attractive regions of selected serotonin receptor binding site using FMO-EDA approach. J Mol Model. 2019 6;25(5):114.
37. Steinmann C, Ibsen MW, Hansen AS, Jensen JH. FragIt: A Tool to Prepare Input Files for Fragment Based Quantum Chemical Calculations. PLoS One. 2012;7(9).
38. Takeda R, Kobayashi I, Suzuki R, Kawai K, Kittaka A, Takimoto-Kamimura M, et al. Proposal of potent inhibitors for vitamin-D receptor based on ab initio fragment molecular orbital calculations. J Mol Graph Model. 2018;80:320–6.
39. Terauchi Y, Suzuki R, Takeda R, Kobayashi I, Kittaka A, Takimoto-Kamimura M, et al. Ligand chirality can affect histidine protonation of vitamin-D receptor: ab initio molecular orbital calculations in water. J Steroid Biochem Mol Biol. 2019;186:89–95.
40. Vuong VQ, Nishimoto Y, Fedorov DG, Sumpter BG, Niehaus TA, Irle S. The Fragment Molecular Orbital Method Based on Long-Range Corrected Density-Functional Tight-Binding. J Chem Theory Comput. 2019;15(5):3008–20.
41. Yoshino R, Yasuo N, Inaoka DK, Hagiwara Y, Ohno K, Orita M, et al. Pharmacophore modeling for anti-Chagas drug design using the fragment molecular orbital method. PLoS One. 2015;10(5):1–15.
42. Willighagen EL, Waagmeester A, Spjuth O, Ansell P, Williams AJ, Tkachenko V, et al. The ChEMBL database as linked open data. J Cheminform. 2013;5(5):1–12.
43. Phillips JC, Braun R, Wang W, Gumbart J, Tajkhorshid E, Villa E, et al. Scalable molecular dynamics with NAMD. J Comput Chem. 2005;26(16):1781–802.
44. Vonommeslaeghe K, Hatcher E, Acharya C, Kundu S, Zhong S, Shim J, et al. CHARMM General Force Field: A Force Field for Drug-Like Molecules Compatible with the CHARMM All-Atom Additive Biological Force Fields. J Comput Chem. 2009;31(4):671–90.
45. Lomize MA, Pogozheva ID, Joo H, Mosberg HI, Lomize AL. OPM database and PPM web server: resources for positioning of proteins in membranes. Nucleic Acids Res. 2012;40(D1):D370–6.
46. Pettersen EF, Goddard TD, Huang CC, Couch GS, Greenblatt DM, Meng EC, et al. UCSF Chimera – A visualization system for exploratory research and analysis. J Comput Chem. 2004;25(13):1605–12.
47. Suenaga M. FACIO. Department of Chemistry, Graduate School of Sciences, Kyushu University, Japan;
48. Fedorov DG, Kitaura K, Li H, Jensen JH, Gordon MS. The polarizable continuum model (PCM) interfaced with the fragment molecular orbital method (FMO). J Comput Chem. 2006 Jun;27(8):976–85.
49. Ballesteros JA, Weinstein H. Integrated Methods for the Construction of Three-Dimensional Models and Computational Probing of Structure-Function Relations in G Protein-Coupled Receptors. Methods Neurosci. 1995;25:366–428.
50. Kurek J, Kwaśniewska P, Myszkowski K, Cofta G. Antifungal , anticancer and docking studies of colchiceine complexes with monovalent metal cation salts. Chem Biol Drug Des. 2019;00:1–14.
51. Kurczab R, Śliwa P, Rataj K, Kafel R, Bojarski AJ. Salt Bridge in Ligand–Protein Complexes—Systematic Theoretical and Statistical Investigations. J Chem Inf Model. 2018;58(11):2224–38.

Supplementary information

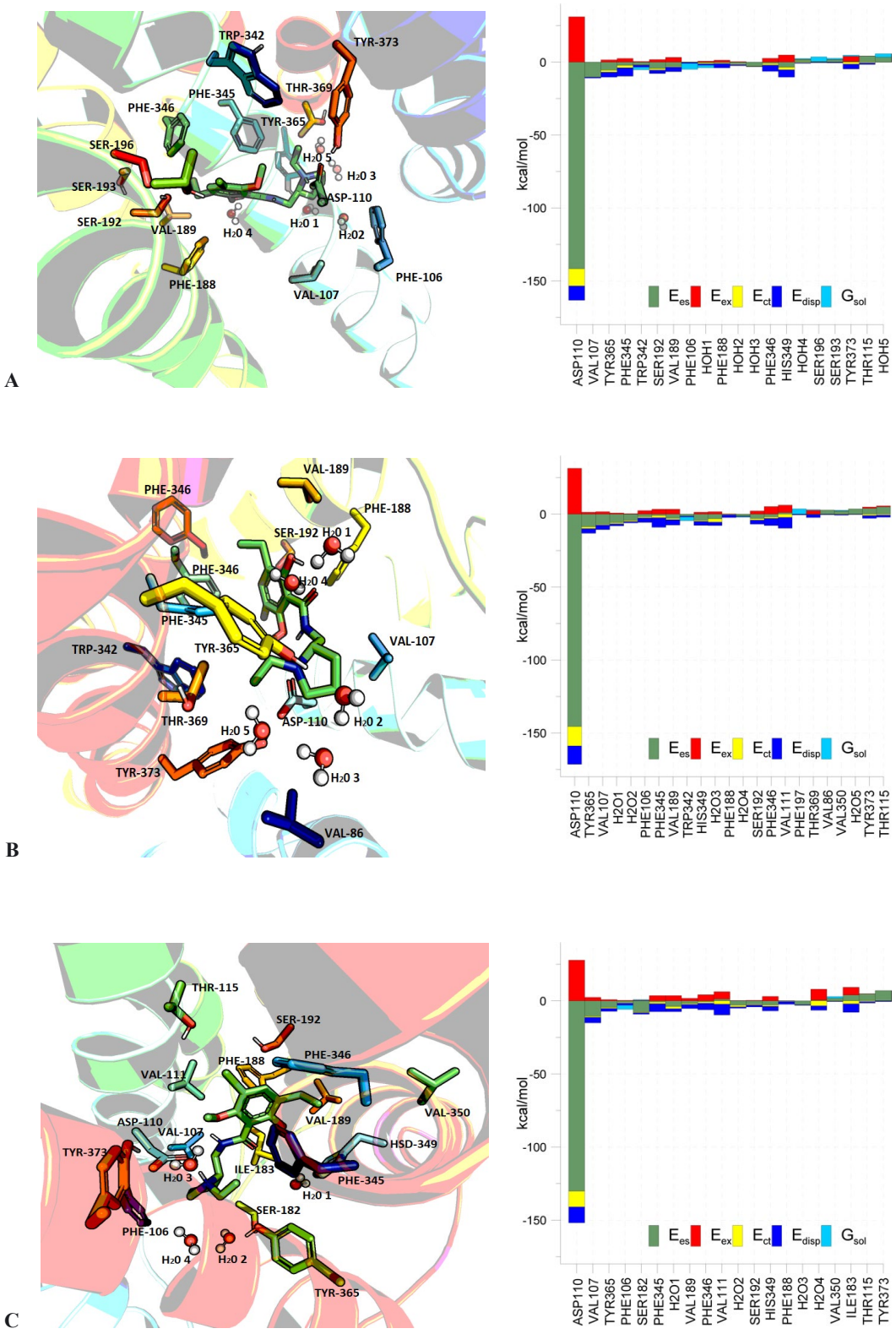

Figure S1. Representation of D3 receptor active sites. Centroids of the first (A), second (B) and third (C) clusters obtained on the basis of the MD trajectory clustering. The FMO-PIEDA energy analysis of those complexes

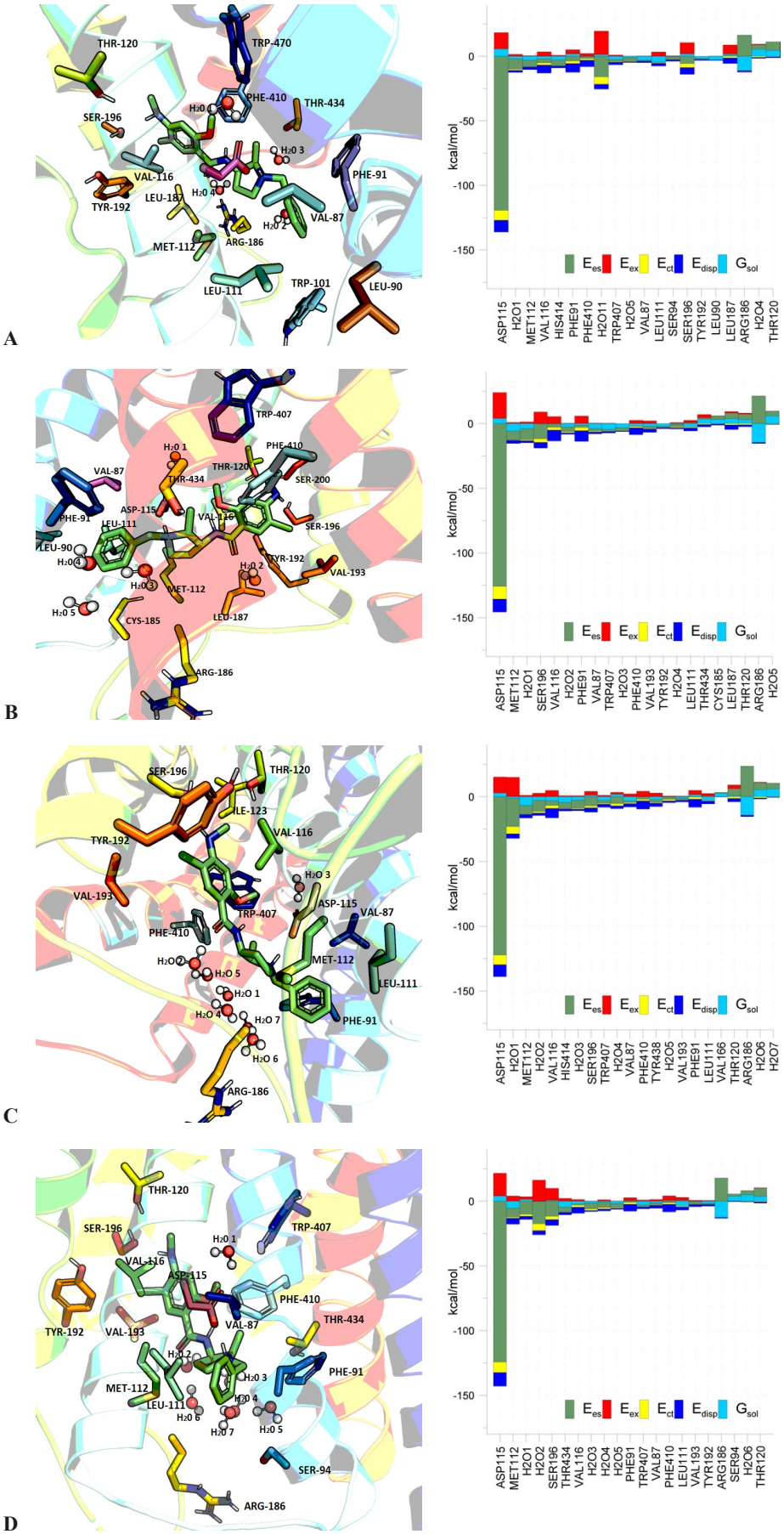

Figure S2. Representation of D4 receptor active sites. Centroids of the first (A), second (B), third (C) and fourth (D) clusters obtained on the basis of the MD trajectory clustering. The FMO-PIEDA energy analysis of those complexes.